Parallel Formulation of the Inverse Kinematics of Modular Hyper-Redundant Manipulators

Gregory S. Chirikjian   Joel W. Burdick

School of Engineering and Applied Science
California Institute of Technology, Mail Code 104-44
Pasadena, CA   91125

Abstract

A 'hyper-redundant' manipulator is a redundant manipulator with a large or infinite relative degree of redundancy. This paper presents a method for generating inverse kinematic solutions for hyper-redundant manipulators of fixed or variable length. This method uses a continuous 'backbone curve' to capture the macroscopic geometric features of the manipulator. The inverse kinematics of the backbone curve can be used directly to specify the geometry of a wide variety of hyper-redundant manipulator morphologies. In this paper hyper-redundant manipulators are broken into non-redundant segments which have closed form inverse kinematic solutions. The kinematic constraints for each segment are specified independently by the backbone curve, and the kinematics of the total manipulator can therefore be solved in parallel. The method is demonstrated with planar and spatial variable geometry truss manipulators.

1. Introduction

Hyper-redundant manipulators have a relative degree of redundancy which is large or infinite. Implementations of hyper-redundant manipulators may consist of truly flexible physical structures such as rubber gas actuator driven devices [4], or the manipulator may consist of a large number of rigid links which approximate a continuous morphology [1,2], or a variable geometry truss [7,8]. 'Hyper-redundant' manipulators, as first referred to in [1], have previously been called 'swan's neck'[5], 'tentacle' [6], and 'highly redundant' [7], among a variety of other names. Applications of hyper-redundant manipulators may include devices for inspection in highly constrained environments [4], novel locomotion devices [3], and articulated space structures [7].

Algorithms for redundant manipulator inverse kinematics generally involve the computation of a Jacobian pseudo-inverse. The computation of a pseudo-inverse becomes prohibitive as the number of manipulator degrees of freedom increases and is impractical for hyper-redundant robots. Special algorithms have been developed for Variable Truss Geometry Manipulators (VGTMs) [7,8]. In those approaches, a continuous curve model was used to describe the macroscopic truss geometry. While that analysis was a big step in demonstrating the use of VGTM's, past work has several drawbacks. First, for spatial manipulators, a curve alone is not sufficient to describe manipulator configuration [2]. Second, unless the curve used to describe the manipulator is parameterized with meaningful physical variables, additional computations are required to specify a desired distribution of actuator displacements. Lastly, while [7,8] deal exclusively with VGTMs, it is not clear how they would apply to other types of hyper-redundant manipulators.

In [1], a method to analyze the kinematics and inverse kinematics of planar continuous and discrete morphology *nonextensible* (fixed-length) hyper-redundant manipulators was presented. This method is based on an intrinsic parameterization of a 'backbone curve,' which captures the macroscopic geometric features of the manipulator, and a modal expansion of the intrinsic curve parameters. Other authors have recently proposed similar ideas for strictly planar manipulators [5,9], while [2] have extended the ideas to 3 dimensions. The work in [2] is extended in this paper to *extensible* manipulators and its application to discretely segmented manipulators is formulated as a parallel algorithm.

The structure of this paper is as follows: Section 2 reviews kinematic methods developed primarily for non-extensible continuous morphology hyper-redundant manipulators and extends the analysis to the case of extensible manipulators. Sections 3 shows how these methods can be implemented as a parallel algorithm and uses the algorithm to solve the inverse kinematics of two particular hyper-redundant manipulators.

2. The Modal Approach to Hyper-Redundant Manipulator Kinematics

This section introduces methods for determining the inverse kinematics of extensible hyper-redundant manipulators. Problems such as noncyclicity and the burdensome computation associated with using pseudo-inverses are circumvented by resolving the hyper-redundancy in ways which lead to closed form inverse kinematic solutions.

2.1 Planar Hyper-Redundant Manipulators

This formulation assumes that the geometric features of any hyper-redundant manipulator without branches or closed loops can be captured by a 'backbone curve.' To describe the planar backbone curve, a frame defining an x_1-x_2 coordinate system is attached to the base of the manipulator. The 'backbone curve' is the locus of all points in the base frame which have position defined by $\overline{x}(s,t) = [x_1(s,t),\ x_2(s,t)]^T$, where $s \in [0,1]$ specifies a point on the manipulator at time $t \in [t_0, t_f]$.

The backbone curve can be parameterized as follows:

$$x_1(s,t) = \int_0^s l(\sigma,t)\sin\theta(\sigma,t)d\sigma \qquad (1a)$$

$$x_2(s,t) = \int_0^s l(\sigma,t)\cos\theta(\sigma,t)d\sigma \qquad (1b)$$

where $l(s,t) = 1 + \epsilon(s,t) > 0$. $\epsilon(s,t)$ describes the local extensibility of the manipulator. For a nonextensible manipulator, $\epsilon(s,t) = 0$, and s becomes the arclength of the backbone curve. $\epsilon(s,t) < 0$ indicates local contraction of the manipulator, while $\epsilon(s,t) > 0$ corresponds to local expansion. The term local indicates that over the length of the manipulator contractions and expansions can occur simultaneously for different values of s.

In this paper we will only consider the case $l(s,t) = l_0(t)$ ($\epsilon(s,t) = l_0(t) - 1$), which corresponds to a uniform extension. $l_0(t_0) = 1$ is the nominal reference configuration. $\theta(s,t)$ is the clockwise measured angle which the tangent to the curve at point s makes with the x_2- axis at time t. Henceforth, the restriction $\theta(0,t) = 0$ is observed.

Forward kinematics can be computed by exact or numerical integration of (1). However, the inverse kinematic problem can have an infinite number of solutions. The complexity of the inverse kinematic problem in the uniform extension case, $l(s,t) = l_0(t)$, can be reduced by specifying:

$$\theta(s,t) = \sum_{i=1}^{N} a_i(t)\Phi_i(s), \qquad (2)$$

which is referred to as modal form, where Φ_i is a *mode function*, and a_i is a time-varying *modal participation factor*. N is the number of modes, which will depend upon the number of end-effector or other task constraints which are specified.

The $\{\Phi_i\}$ are specified functions, and thus the inverse kinematics problem is reduced to finding the $\{a_i\}$ which satisfy the end effector constraints when the desired length, l_0, has been specified. When N is the same as the number of specified end-effector degrees of freedom, inverse kinematic solutions based on the modal approach in (2) serve as a means of 'hyper-redundancy resolution' to within a choice of manipulator length. l_0 parameterizes the remaining redundancy directly in closed form. The method is cyclic because the choice of modes, $\{\Phi_i\}$ (which must satisfy nondegeneracy conditions [2]), and number of modes, N, uniquely specifies the effective number of degrees of freedom of the manipulator, for a specified manipulator length.

For some choices of modes, exact inverse kinematic solutions can be found, one of which is presented below. Consider the following choice of modes for $N = 2$:

$$\Phi_1(s) = \sin 2\pi s; \qquad \Phi_2(s) = 1 - \cos 2\pi s. \qquad (3)$$

Substituting these two modes into (1-2) and evaluating at $s = 1$,(which is the point on the manipulator located at the end-effector), it can be shown that the forward kinematics equations reduce to

$$x_1(1,t) = l_0 \sin(a_2) J_0\left[(a_1^2 + a_2^2)^{\frac{1}{2}}\right] \qquad (4a)$$

$$x_2(1,t) = l_0 \cos(a_2) J_0\left[(a_1^2 + a_2^2)^{\frac{1}{2}}\right] \qquad (4b)$$

where J_0 is the zeroth order Bessel function. The 'inverse kinematics' (evaluation of modal participation factors) for the case $l_0 = 1$ has been computed in [1]. It should be noted that whenever an inverse kinematics solution can be found for a nonextensible manipulator of the form $\overline{a} = \overline{f}^{-1}(\overline{x}(1,t))$, the inverse kinematic solution of the uniformly extensible case will be $\overline{a} = \overline{f}^{-1}(\overline{x}(1,t)/l_0)$, as can be seen by comparing Equation (1) evaluated with $l(s,t) = 1$ and $l(s,t) = l_0(t)$ respectively. This means that other inverse kinematics solution presented in previous work [2] can be used for the solution of both nonextensible and extensible manipulators. While it is desirable to have closed form solutions for the backbone curve inverse kinematics, it is not a necessity. For instance, resolved rate formulations can be used with the participation factors as the generalized coordinates. Alternately, the backbone

curve forward kinematics can be computed numerically to generate a look-up table relating end-effector coordinates to participation factors.

2.2 Spatial Hyper-Redundant Manipulators

Every point on the backbone curve of a spatial hyper-redundant manipulator can be represented by the parametric equations:

$$\overline{x}(s,t) = \begin{pmatrix} \int_0^s l(\sigma,t)\sin K(\sigma,t)\cos T(\sigma,t)d\sigma \\ \int_0^s l(\sigma,t)\cos K(\sigma,t)\cos T(\sigma,t)d\sigma \\ \int_0^s l(\sigma,t)\sin T(\sigma,t)d\sigma \end{pmatrix} . \quad (5)$$

This form is not unique and was chosen so that when $T(s,t) = 0$ for all s,t, the spatial case degenerates to the planar case. By convention, $K(0,t) = T(0,t) = 0$.

A frame can be assigned to every point on a space-curve defined by the parameters K, and T. This frame, referred to as the *nominal reference frame* is denoted by the triplet of vectors $\{\overline{\Psi}_1(s,t),\overline{\Psi}_2(s,t),\overline{\Psi}_3(s,t)\}$:

$$\overline{\Psi}_2 = \frac{1}{l}\frac{\partial\overline{x}}{\partial s}; \qquad \overline{\Psi}_3 = \frac{\partial\overline{\Psi}_2}{\partial T}; \qquad \overline{\Psi}_1 = \frac{1}{\cos T}\frac{\partial\overline{\Psi}_2}{\partial K} \quad (6)$$

and are respectively termed the *tangent, complementary* vector, and *planar-normal*.

The orientation of the nominal reference frame at point s and time t with respect to the fixed frame at the origin is given by the matrix

$$[\Psi(s,t)] = \left[\overline{\Psi}_1(s,t),\overline{\Psi}_2(s,t),\overline{\Psi}_3(s,t)\right] . \quad (7)$$

Unlike the planar case, the geometry of spatial hyper-redundant manipulators is not completely specified by the curve representation. The function called the *roll distribution*, $R(s,t)$, is also required to specify the spatial hyper-redundant manipulator configuration. $R(s,t)$ is defined as follows: A frame denoted $\{F_R(s,t)\}$, and termed the *body fixed frame*, is initially coincident with the nominal reference frame for all s. The unit basis vectors of $\{F_R(s,t)\}$ are given by: $\{\overline{\Xi}_1(s,t),\overline{\Xi}_2(s,t),\overline{\Xi}_3(s,t)\}$, where $\overline{\Xi}_2(s,t) = \overline{\Psi}_2(s,t)$. The roll distribution is the angle defined by

$$R(s,t) = \cos^{-1}\left(\overline{\Xi}_1(s,t)\cdot\overline{\Psi}_1(s,t)\right), \quad (8)$$

and measures how much the body fixed frame twists along the manipulator backbone curve with respect to the nominal reference frame. By convention, $R(0,t) = 0$.

The modal method can be used to formulate spatial hyper-redundant manipulator kinematic algorithms :

$$K(s,t) = \sum_{i=1}^{N_K} a_i(t)\Phi_i(s); \quad T(s,t) = \sum_{i=1}^{N_T} \alpha_i(t)\Gamma_i(s)$$
$$(9a)$$

$$R(s,t) = \sum_{i=1}^{N_R} \beta_i(t)\Delta_i(s). \quad (9b)$$

5 modal participation factors, distributed between $\{a_i\}$ and $\{\alpha_i\}$, and at least a one parameter roll distribution, determined by specifying $\{\beta_i\}$, are generally sufficient to solve spatial position and orientation problems, with l_0 parameterizing a free degree of freedom. Solution techniques for the inverse kinematics of a spatial backbone curve are essentially the same as for the planar case.

3. Inverse Kinematics in Parallel

A parallel algorithm based on the kinematic formulation of the previous section is introduced here. For the sake of simplicity, manipulators with a modular architecture are considered. For example, the modules of an extensible spatial hyper-redundant manipulator might be Stewart platforms. It is assumed that the modules are uniform in structure and size, although this is not necessary.

The continuous curve kinematic solutions can be used to generate the inverse kinematic solution for modular manipulators as follows. Consider the ith module in the manipulator chain consisting of n modules. Attach a frame, $\{F_{i-1}\}$, to the 'input', or base, of the module, and a frame, $\{F_i\}$, to the 'output', or top, of the module. To have the discretely segmented modular manipulator configuration conform to the continuous curve geometry, the frames $\{F_{i-1}\}$ and $\{F_i\}$ are chosen to coincide with the body fixed frames of the continuous curve at points given by $s = (i-1)/n$ and $s = i/n$ respectively.

The 4×4 homogeneous transform relating $\{F_i\}$ to $\{F_{i-1}\}$ is denoted by $\mathbf{H}_{i-1}^i$. This consists of the relative translation, $\overline{r}_{i-1}^i$ and rotation, $[Q]_{i-1}^i$, of $\{F_i\}$ with respect to $\{F_{i-1}\}$, i.e.,

$$\mathbf{H}_{i-1}^i = \begin{pmatrix} [Q]_{i-1}^i & \overline{r}_{i-1}^i \\ \overline{0}^T & 1 \end{pmatrix} . \quad (10)$$

It is assumed that the inverse kinematics of the module, which relate $\{F_i\}$ to $\{F_{i-1}\}$, can be solved in a closed or efficient form. Equation (10) supplies, as a

function of the modal participation factors, the input to the inverse kinematics of each module.

The discrete manipulator configuration will conform to the continuous curve model by setting :

$$[Q(t)]^i_{i-1} = [A((i-1)/n, t)]^T [A(i/n, t)] \qquad (11)$$

and

$$\bar{r}(t)^i_{i-1} = [A((i-1)/n, t)]^T (\bar{x}(i/n, t) - \bar{x}((i-1)/n, t)) \qquad (12)$$

where:

$$[A(s, t)] = \text{ROT}[\bar{\Psi}_2(s, t), R(s, t)][\Psi(s, t)] \qquad (13)$$

is the rotation matrix relating the orientation of the body fixed frame with unit vectors $\{\bar{\Xi}_i(s, t)\}$ at point s to the base frame at $s = 0$. The notation $ROT[\bar{v}, w]$ indicates a rotation about the vector $\bar{v}$ by an amount w (using the right hand rule). In other words, $[A(s, t)]$ describes the orientation of the frame $\{F_R(s, t)\}$ with respect to the base frame. $[A(s, t)]$ is a composition of rotations from the base frame to the nominal reference frame, and a rotation due to the roll distribution. In this way, the frames fixed in the discrete manipulator, $\{F_i(t)\}$, coincide with the body fixed frames, $\{F_R(i/n, t)\}$, defined for the continuous backbone at the discrete points $s = i/n$ for all $i \in [0, n]$. In the planar case $T(s, t) = R(s, t) = 0$ for all s, t, and the above equations reduce to:

$$\bar{r}^i_{i-1} = l_0 \begin{pmatrix} \int_{\frac{i-1}{n}}^{\frac{i}{n}} \sin[\theta(s, t) - \theta(\frac{i-1}{n}, t)]ds \\ \int_{\frac{i-1}{n}}^{\frac{i}{n}} \cos[\theta(s, t) - \theta(\frac{i-1}{n}, t)]ds \\ 0 \end{pmatrix} . \qquad (14)$$

and

$$[Q]^i_{i-1} = \text{ROT}\left[-\bar{e}_3, \theta\left(\frac{i}{n}, t\right) - \theta\left(\frac{i-1}{n}, t\right)\right] \qquad (15)$$

where $\bar{e}_3 = [0, 0, 1]^T$.

Once the backbone curve inverse kinematic solution has been computed, each $[Q]^i_{i-1}$ and $\bar{r}^i_{i-1}$ can be computed in parallel. Similarly, the inverse kinematics of each module can also be performed in parallel, and this method can in theory be applied to manipulators with an arbitrary number of degrees of freedom with the same computation time. This method is applicable to a wide variety of morphologies. The following sections present two examples which illustrate the theory.

3.1 A Planar Truss Manipulator

Figure 1 shows one module of a planar truss manipulator. In this case, one segment of the truss is composed of side members and a cross element. The position vector connecting like vertices in the truss are denoted $\bar{v}^i_0$ on the left and $\bar{v}^i_1$ on the right. $\bar{c}^i$ denotes the cross element. These vectors can be determined from the continuous curve model as follows:

$$\bar{v}^i_j = \bar{r}^i_{i-1} - \bar{n}^i_j + \text{ROT}(-\bar{e}_3, \theta^i_{ee})\bar{n}^i_j \qquad j = 1, 2$$
$$\bar{c}^i = \bar{r}^i_{i-1} - \bar{n}^i_1 + \text{ROT}(-\bar{e}_3, \theta^i_{ee})\bar{n}^i_2 \qquad (16)$$

where $\theta^i_{ee} = \theta(i/n, t) - \theta((i-1)/n, t)$ and $\bar{n}^i_j$ are the vectors to the jth vertex of the ith platform in the frame affixed to that platform. For this specific example, $\bar{n}^i_1 = [-w_0/2, 0]^T$ and $\bar{n}^i_2 = [w_0/2, 0]^T$ where w_0 is the width of each horizontal face of the truss.
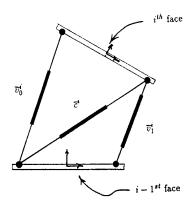

Figure 1: One Section of a Planar Truss Manipulator

The controlled degrees of freedom are the lengths

$$\lambda^i_j = ||\bar{v}^i_j||; \qquad \lambda^i_3 = ||\bar{c}^i|| \qquad (17)$$

for $i = 1, ..., n$, and $j = 1, 2$. Thus, (16) and (17) provide the inverse kinematics solution for this module geometry based on the backbone curve geometry.

We now use the $\theta(s, t)$ function of the example presented in [1] to demonstrate how the geometry of a truss manipulator could be specified in an obstacle field. For this example the manipulator is restricted to be locally nonextensible so $l_0(t) = 1$, even though the physical structure allows extension and contraction. The objective in this example, as seen in Figure (2b), is to navigate the manipulator through the obstacle field with dimensions specified in Figure (2a).
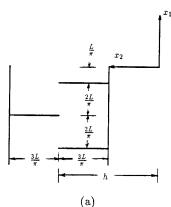
One way to achieve this is to define :

$$\theta(s,t) = J_0^{-1}\left(\frac{h}{s_1}\right)\sin\left(\frac{2\pi s}{s_1}\right) - \pi W(s, s_1 + 3L, 1).$$

$$- \frac{\pi}{L}(s - s_1)W(s, s_1, s_1 + L)$$

$$+ [\frac{\pi}{L}(s - s_1 - L) - \pi]W(s, s_1 + L, s_1 + 2L)$$

$$- \frac{\pi}{L}(s - s_1 - 2L)W(s, s_1 + 2L, s_1 + 3L)$$

$$(18)$$

where the window functions $W(s, a, b)$ simply take the value of 1 when $a \leq s < b$ and zero otherwise. s_1 is the length of the manipulator backbone curve outside of the obstacle field. h is the distance between the manipulator base and the entrance to the obstacle, and L is defined in Figure 2(a). The details of how Equation (18) was derived can be found in [1]. In Figure 2(b) The width of the truss is taken as $w_0 = 0.053$, and the number of bays in the truss is $n = 15$ with the values $s_1 = 1.0, 0.793, 0.607$.
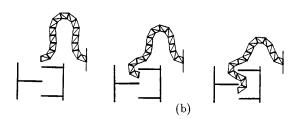

(a)

(b)

Figure 2: Truss Manipulator In an Obstacle Field

3.2 A Spatial Truss Manipulator

Figure 3 shows the geometry of one story, or bay, of an articulated spatial truss structure previously examined in [7,8]. The geometry of the base and top faces of each truss segment is fixed, and the vertical and diagonal elements can expand and contract. Because the

elements are connected with passive ball joints there are no constraint equations involved and the dimensions of the six actuators define the position and orientation of the top face with respect to the bottom.
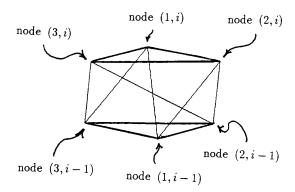

Figure 3: One Story of a Highly Articulated Structure

The module inverse kinematics problem reduces to the determination of the lengths of the truss elements which cause the manipulator to conform to the backbone curve. The lengths of the truss elements required to generate a position and orientation of the ith face relative to the $i - 1^{st}$ face can be determined as follows. Denote the position vector from node $(j, i-1)$ to node (j, i) by $\overline{v}_j^i$ for $j = 1, 2, 3$. These vectors are defined in the body fixed frame $\{F_{i-1}\}$, and can be computed as:

$$\overline{v}_j^i = \overline{r}_{i-1}^i + ([Q]_{i-1}^i - [I])\overline{n}_j. \tag{19}$$

$\overline{n}_j$ are the vectors to the vertices in the frame affixed to the center of each face, which is defined by the unit vectors $\{\overline{\Xi}_i\}$. For the particular example given, these vectors are

$$\overline{n}_1 = w_1[1, \ 0, \ 0]^T$$

$$\overline{n}_2 = w_1[-\sin\pi/6, \ 0, \ -\cos\pi/6]^T$$

$$\overline{n}_3 = w_1[-\sin\pi/6, \ 0, \ \cos\pi/6]^T$$

where w_1 determines the width of the truss. The three cross elements are each denoted by $\overline{c}_j^i$ for $j = 1, 2, 3$. They have the explicit form:

$$\overline{c}_1^i = \overline{r}_{i-1}^i - \overline{n}_1 + [Q]_{i-1}^i \overline{n}_2 \qquad (20a)$$

$$\overline{c}_2^i = \overline{r}_{i-1}^i - \overline{n}_2 + [Q]_{i-1}^i \overline{n}_3 \qquad (20b)$$

$$\overline{c}_3^i = \overline{r}_{i-1}^i - \overline{n}_3 + [Q]_{i-1}^i \overline{n}_1. \qquad (20c)$$

The actuatable degrees of freedom are the magnitudes of each of these vectors. These are denoted by λ_j^i, where

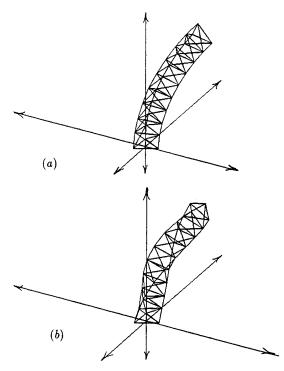$$\lambda_j^i = ||\overline{v}_j^i||; \qquad \lambda_{j+3}^i = ||\overline{c}_j^i||. \tag{21}$$

gramming of these devices arising from their non-anthropomorphic geometry. The algorithms developed in this paper are a step toward efficient kinematic control of hyper-redundant robots. Challenging work in mechanical implementation and high performance control algorithms still remain.

Aknowledgements

5. References

[1] Chirikjian, G.S., Burdick, J.W., "An Obstacle Avoidance Algorithm for Hyper-Redundant Manipulators," *1990 IEEE Conference on Robotics and Automation*, Cincinnatti, Oh, May 14-17, 1990.

[2] Chirikjian, G.S., Burdick, J.W., "Kinematics of Hyper-Redundant Manipulators," *ASME Mechanisms Conference*, Chicago, Il, Sept. 16-19, 1990.

[3] Chirikjian, G.S., Burdick, J.W., "Kinematics of Hyper-Redundant Robot Locomotion with Applications to Grasping," *1991 IEEE Conference on Robotics and Automation*

[4] Fukuda, T., Hosokai, H., Uemura, M., " Rubber Gas Actuator Driven by Hydrogen Storage Alloy for In-pipe Inspection Mobile Robot with Flexible Structure," *Proceedings 1989 IEEE Conference*, May. 1989, pp. 1847-1852.

[5] Hayashi, A., Park, J., Kuipers, B.J., "Toward Planning and Control of Highly Redundant Manipulators," *Fifth IEEE International Symposium on Intelligent Control, 1990*.

[6] Ivanescu, M., Badea, I.,"Dynamic Control for a Tentacle Manipulator," Int. Conf. on Robotics and Factories of the Future, pp. 317-328, Dec 4-7, 1984, Charlotte, Nc, USA.

[7] Naccarato, F., Hughes, P.C., "An inverse Kinematics Algorithm for A Highly Redundant Variable-Geometry-Truss Manipulator," *Proceedings of the 3rd Annual Conference on Aerospace Computational Control*, ed. by D.E. Bernard and G.K. Man, Oxnard, CA, JPL Publication 89-45, Dec. 15, 1989.

[8] Salerno, R.J., Reinholtz, C.F., Robertshaw, H.H., "Shape Control of High Degree-of-Freedom Variable Geometry Trusses," *Proceedings of the Workshop on Computational Aspects in the Control of Flexible Systems, part 2*, Williamsburg, VA, July 12-14, 1988.

[9] Tavakkoli, S., Dhande, S.G., "Shape Synthesis and Optimization Using Intrinsic Geometry" *Proceedings of the ASME Design Conference*, Chicago, Il, Sept. 16-19, 1990.

Figure 4: Two Configurations with the Same Backbone Curve

Figure 4 shows a VGTM with 9 bays, $l_0 = 1$, and $w_1 = 0.1$. In this example $N_K = 3$, $N_T = 2$, and $N_R = 1$ and the modes used are $\Phi_1(s) = \Gamma_1(s) = \Delta_1(s) = s$, $\Phi_2(s) = \Gamma_2(s) = 1 - \cos 2\pi s$, and $\Phi_3(s) = \sin 2\pi s$. The inverse kinematics of this example has not been solved in closed form. Figure 4(a) shows the configuration corresponding to the participation factors $(a_1, a_2, a_3) = (0.6, 0, 0)$, $(\alpha_1, \alpha_2) = (-1.2, 0)$, and $\beta_1 = 0$. This corresponds to a position of $(0.19, 0.74, -0.53)$, and direction cosines of the tangent to the backbone curve at the end-effector of $(0.21, 0.30, -0.93)$. The only difference between Figures 4(a) and (b) is that in Figure 4(b), $\beta_1 = 3.0$. This example demonstrates that even though two VGTs may have identical backbone curves, the manipulator configuration is not fully specified until the roll distribution is defined.

4. Conclusions

This paper has generalized the kinematic methods developed in [1,2] to extensible manipulators. Application of the method as a parallel algorithm was explained. Hyper-redundant robots have failed to achieve wide-spread applicability due to inefficiency and ineffectiveness of previous kinematic modeling techniques, complex mechanical design, and complexity in the pro-